Cytokinesis defines a spatial landmark for hepatocyte polarization and apical lumen formation

Ting Wang[1], Kilangsungla Yanger[2], Ben Z. Stanger[1,2], Doris Cassio[3], and Erfei Bi[1,*]

[1]Department of Cell and Developmental Biology, Perelman School of Medicine, University of Pennsylvania, Philadelphia, PA 19104, USA

[2]Gastroenterology Division, Department of Medicine, Perelman School of Medicine, University of Pennsylvania, Philadelphia, PA 19104, USA

[3]INSERM, UMR-S 757, Université Paris-Sud, Orsay, F-91405, France

*Corresponding author:

Erfei Bi, Ph.D.

Department of Cell and Developmental Biology

Perelman School of Medicine

University of Pennsylvania

Room 1156, BRB II/III

421 Curie Blvd

Philadelphia, PA 19104-6058

Tel: 215-573-6676

Fax: 215-898-9871

Email: ebi@mail.med.upenn.edu

JCS Advance Online Article. Posted on 4 April 2014

Summary

By definition, all epithelial cells have apical-basal polarity, but it is unclear how epithelial polarity is acquired and how polarized cells engage in tube formation. Here, we show that hepatocyte polarization is linked to cytokinesis using the rat hepatocyte cell line Can 10. Before abscission, polarity markers are delivered to the site of cell division in a strict spatiotemporal order. Immediately after abscission, daughter cells remain attached through a unique disc-shaped structure, which becomes the site for targeted exocytosis, resulting in the formation of a primitive bile canaliculus (BC). Subsequently, oriented cell division and asymmetric cytokinesis occur at the BC midpoint, resulting in its equal partitioning into daughter cells. Finally, successive cycles of oriented cell division and asymmetric cytokinesis lead to the formation of a tubular bile canaliculus (tBC) shared by two rows of hepatocytes. These findings define a novel mechanism for cytokinesis-linked polarization and tube formation, which appears to be broadly conserved in diverse cell types.

Introduction

Epithelial tissue lines body surfaces and cavities and thus plays critical roles in a variety of functions including protection, secretion, selective absorption, and gas exchange (Datta et al., 2011; Hogan and Kolodziej, 2002; Lubarsky and Krasnow, 2003; Rodriguez-Fraticelli et al., 2011). Epithelial tissue consists of one or more layers of polarized cells that are connected via junctional complexes (tight junctions, adherens junctions, desmosomes, and GAP junctions), which enables them to act as a structural and functional unit. Epithelial cells are commonly organized into tubes of different sizes and shapes, with their apical domains facing the lumen and their basal domains facing the underlying connective tissue, and several mechanisms involved in tube formation have been described (Datta et al., 2011; Hogan and Kolodziej, 2002; Lubarsky and Krasnow, 2003).

The mechanisms underlying epithelial cell polarization and apical lumen formation are not well understood. Studies using 2D cell models such as Madin-Darby Canine Kidney (MDCK) cells suggest that cell-cell adhesion triggers polarization (McCaffrey and Macara, 2012; St Johnston and Ahringer, 2010) while emerging evidence from studies involving 3D cultures of MDCK and human intestinal Caco-2 cells suggests that polarization and apical lumen formation are associated with cell division (Jaffe et al., 2008; Schluter et al., 2009; Tawk et al., 2007). However, it remains unknown whether division-linked polarization defines a general mechanism for epithelial polarization and whether this mechanism can explain physiologically relevant tissue architecture and function.

Hepatocytes, the major parenchymal cells of the liver, are specialized epithelial cells. These cells perform vital functions in humans and other vertebrates including detoxification, synthesis of serum proteins, metabolism, and bile production (Decaens et al., 2008; Wang and Boyer, 2004). Within the liver, hepatocytes are organized into cords in which two rows of cells share a central apical lumen called the bile canaliculus (BC), a specialized tubule into which bile acids and the products of hepatic detoxification are excreted and transported to the small intestine. The basal surfaces of the hepatocytes are adjacent to blood vessels where

serum proteins and hormones produced by the hepatocytes enter the circulation. Thus, the architecture and function of the liver depends critically on hepatocyte polarization and organization. While other aspects of hepatocyte polarization, such as membrane trafficking and BC formation, have been studied extensively in primary hepatocytes and various cell lines (Tuma et al., 1999; Tuma et al., 2001; Wakabayashi et al., 2005; Wang and Boyer, 2004; Zegers and Hoekstra, 1998), the spatiotemporal trigger for the initial polarization of hepatocytes and the mechanism underlying BC formation and tubulogenesis in the liver remain unknown.

In this study, using the rat hepatocyte cell line Can10 that polarizes and forms BC robustly *in vitro* (Treyer and Musch, 2013; Decaens et al., 2008; Peng et al., 2006), we found that hepatocyte polarization and apical lumen formation are linked to cytokinesis. In addition, we found that oriented cell division is associated with BC formation *in vivo*. Our study, together with existing evidence, suggests that cytokinesis-linked polarization is broadly conserved in diverse cell types.

Results

Hepatocyte polarization and apical lumen formation are spatially linked to cytokinesis

To determine how hepatocytes become polarized, we observed individual Can 10 cells by time-lapse microscopy. Strikingly, most cells (23 out of 26) did not undergo complete abscission after cytokinesis (**Fig. 1A; See Movie 1 in supplementary material**). Instead, the daughter cells remained attached and a small BC-like structure appeared at the division site (**Fig. 1A, arrow**). This structure was clearly observable 2 – 8 h after cytokinesis by phase-contrast microscopy and became enlarged over time. The canalicular nature of the structure was confirmed by live-cell imaging followed by fixation and staining of the imaged cells for Mdr (ABCB1, ATP Binding Cassette, sub-family B, member 1), an authentic BC membrane marker (Peng et al., 2006) (**Fig. 1B, arrows; See Movie 2 in supplementary material**). In a few cells (2 out of 23), the BC structure was eventually split into two spheres at the division site, which were subsequently endocytosed (**See Movie 3 in supplementary material**). Together, our data suggest that hepatocyte polarization and apical lumen formation are spatially linked to cytokinesis.

Polarity regulator, tight junction-associated protein, and apical membrane marker localize to the division site in distinct spatiotemporal patterns

To determine how hepatocyte polarization and apical lumen formation are linked to cytokinesis at the molecular level, we monitored the localization of Par3 (a key regulator of epithelial cell polarity) (Martin-Belmonte and Mostov, 2008; St Johnston and Ahringer, 2010), ZO-1 (a tight junction-associated protein), and Mdr during the cell division cycle (**Fig. 1C**). The late stages of cytokinesis were visualized by staining for Aurora B, a protein kinase that localizes to the central spindle in anaphase and remains on the opposing microtubule (MT) arrays that overlap at the midbody before abscission (Delacour-Larose et al., 2004; Gruneberg et al., 2004; Murata-Hori et al., 2002). It became immediately clear that the polarity proteins and BC markers localize to the division site in a strict order (Par3 → ZO-1 → Mdr) and with distinct patterns (**Fig. 1C**). Par3 first localized near the MT plus ends sandwiching the midbody (**Fig. 1C, top left, arrows**), and then relocated to the plasma membrane (PM) at the

division site during late midbody stage, which was indicated by the pair of tiny Aurora B "bars" (**Fig. 1C, top right**). Importantly, 93% of the cells (n = 44) containing a pair of Aurora B bars showed Par3 localization at the division site (near the midbody or on the PM). In contrast, ZO-1 did not associate with the MT plus ends during early midbody stage (**Fig. 1C, middle left**) but did localize to the PM at the division site during late midbody stage (**Fig. 1C, middle right**). However, only 47% of the cells (n = 58) containing a pair of Aurora B bars showed this type of localization. Strikingly, Mdr localized near the minus ends of the MT arrays but not on the PM at the division site. This pattern of localization was particularly apparent during late midbody stage (**Fig. 1C, bottom right**). However, only 25% of the cells (n = 138) containing a pair of Aurora B bars showed such localization. Together, these data indicate that a key polarity regulator, a tight junction-associated protein, and a BC membrane marker are delivered to the division site in distinct spatiotemporal patterns before abscission, and also suggest that hepatocytes begin to polarize at the time of cytokinesis prior to lumen formation.

Assembly and subsequent opening of a disc-shaped tight junction at the division site is accompanied by the emergence of an apical lumen

Our time-lapse analysis indicated that an apical lumen or nascent BC was formed and enlarged over time at the division site between the divided yet still attached daughter cells (**Fig. 1A; See Movie 1 in supplementary material**). BC formation likely occurs after cytokinesis (defined as the separation of cytoplasm between the daughter cells), as this process was never observed in cells still containing detectable Aurora B bars. To understand the molecular underpinnings of BC formation, we divided the process into three stages: pre-BC, small-BC, and large-BC, and monitored the key molecular events associated with cell polarization and membrane trafficking at each of these stages (**Fig. 2**). We found that at the pre-BC stage, the tight junction-associated protein (ZO-1) and actin filaments (F-actin) co-localized between the two daughter cells as a "round disc" and the apical vesicles (Mdr) had an intracellular localization that was in close proximity to the disc (**Fig. 2A, top**). At the small-BC stage, a clear space formed in the center of the round disc, which is likely caused by targeted exocytosis of apical vesicles (**cf. Fig. 5**), resulting in the formation of a ring-like tight junction (**Fig. 2A, middle**).

This interpretation is supported by the observation that the exocyst (as indicated by its subunit Exo70), a multi-protein complex required for vesicle tethering at the PM (He and Guo, 2009; Novick and Guo, 2002), localized to the center of the tight-junction disc at the pre-BC stage (**Fig. 2B, top**), and closely associated with the BC membrane at the small-BC stage (**Fig. 2B, middle**). The basic architecture of a large BC was very similar to that of a smaller one (**Fig. 2A, B; compare bottom to middle**), with the enlargement of the BC presumably caused by continued exocytosis (**cf. Fig. 5**). Basolateral proteins such as β-catenin was clearly segregated from the apical proteins during the small-BC stage and thereafter (data not shown). Strikingly, Par3 displayed perfect co-localization with ZO-1 during each stage of BC formation (**Fig. 2C**), suggesting its involvement in tight junction assembly, as demonstrated in other epithelial cells (Helfrich et al., 2007; Hirose et al., 2002). Together, these data suggest that tight junction assembly and targeted exocytosis at the division site may play a critical role in BC formation.

Oriented cell division and asymmetric cytokinesis are associated with apical tube formation

Within the liver, the BC formed by two adjacent hepatocytes is part of a tubular BC (tBC) shared by two rows of hepatocytes. To understand how the tBC arises from the BC formed at the two-cell stage, we examined the next round of cell division in Can 10 cells already harboring a BC structure. Strikingly, in cells with a preexisting BC and a mitotic spindle, the spindle was oriented approximately in parallel to the long axis of the preexisting BC in 71% (n = 75) of the cells (**Fig. 3A**). In addition, the cleavage furrow, which is perpendicular to the mitotic spindle, ingressed asymmetrically towards the preexisting BC (**Fig. 3B**). Together, these data indicate that oriented cell division and asymmetric cytokinesis are associated tBC formation.

Consistent with the conclusion reached above, we found that in 75 ± 10% (n = 126) of the Can 10 cells containing both a midbody and a BC, the midbody was closely associated with the BC membrane (**Fig. 3C, D; cf. Fig. 4E**). Moreover, the BC membrane was constricted at the midbody position (**Fig. 3C**), suggesting that the preexisting or the "mother" BC is

incompletely divided by the contractile actomyosin ring and partitioned into the daughter cells. This suggestion is further supported by our observation that the circle of tight junctions surrounding the mother BC was also pulled inward at the division site (**Fig. 3D**), presumably by the same contractile force, resulting in the formation of two "lasso-shaped" tight junctions. As new tight junctions are expected to assemble at the division site followed by BC formation within the junctions at the two-cell stage (**Figs. 1C; 2A, B**), the newly formed junctions and BC at the three-cell or later stages must join the old ones to form a more complex network of junctions surrounding a single BC lumen (**See Movie 4 in supplementary material**). Together, these data suggest that cytokinesis-coupled partitioning of the mother BC into the daughter cells and the further growth of the existing BC may lead to tBC formation.

To determine whether tBC is formed by a similar mechanism *in vivo*, we examined the spatial relationship between cell division and the existing BC in mouse liver sections from E16.5 to 17.5, which covers the developmental period for active BC biogenesis (Kung et al., 2010; Navarro-Alvarez et al., 2010). Because of the difficulty in distinguishing true fluorescence signal at the two-cell stage from background noise in the liver sections (both were small puncta or tiny bands in appearance), we could not decipher the mechanism of hepatocyte polarization and BC formation at this stage. However, we could determine the association of a pair of Aurora B bars with a tBC with clarity. We found that whenever a clear midbody and a tBC were observed in the same area, they were always closely associated with each other and never separated by any detectable distance (100%, n = 40) (**Fig. 3E**). Thus, tBC formation appears to be dictated by a similar mechanism *in vivo*.

Par3 is required for tight-junction assembly, and the emergence and expansion of an apical lumen

Our observation that Par3 localizes to the division site before the completion of cytokinesis and to the tight junction during BC formation suggests that Par3 may define a molecular link between cytokinesis and apical lumen formation. To examine this possibility, we performed siRNA-mediated knockdown of Par3, and found that the knockdown did not affect overall cell proliferation but significantly impaired BC formation (**Fig. 4A**). The percentage of cells

engaged in BC formation was reduced from 80 ± 2% (n = 1781 from 3 independent experiments) for the control (siCon) cells to 66 ± 4% (n = 1169 from 3 independent experiments) for the siPar3 cells (p = 0.0045) (**Fig. 4B, left**). Par3 knockdown also caused a significant reduction in the average length per BC, going from 13 ± 10 μm for the siCon cells (645 BCs for the 1781 cells) to 10 ± 5 μm for the siPar3 cells (318 BCs for the 1169 cells) (p < 0.001) (**Fig. 4B, right**). These phenotypes were confirmed using a different siRNA against Par3 (**supplementary material Fig. S1**). The remaining BCs observed in the siPar3 cells may reflect an incomplete depletion of Par3 (**Fig. 4D; supplementary material Fig. S1D**), a preferential requirement of Par3 for BC formation but not maintenance (**supplementary material Fig. S1E**), and/or the involvement of additional mechanism acting in parallel to Par3. Regardless, these data indicate that Par3 plays a significant role in BC formation as well as its expansion.

As Par3 displays perfect co-localization with ZO-1 throughout BC formation (**Fig. 2C**), we thought that Par3 might control BC formation by regulating tight-junction assembly. To test this possibility, we examined tight-junction assembly in Par3-knockdown and control cells. Strikingly, tight junctions associated with the "early stage" of BC formation (see figure legend for more explanations) were reduced from 31% (n = 109 cell pairs) in the control cells to 10% (n = 71) in the siPar3 cells (**Fig. 4C**). In contrast, the tight junctions associated with the later stage of BC formation remained high in siPar3 cells (90% vs. 69% in the control cells) (**supplementary material Fig. S1F**). These data indicate that Par3 is required for the *de novo* assembly of a tight junction at the division site, and is less critical for the maintenance of a mature tight junction.

As shown early (**Fig. 3**), tBC formation involves the association between a midbody and a preexisting BC. Strikingly, such an association was significantly reduced in the siPar3 cells (23 ± 3.0%, n = 90) as opposed to the control cells (75 ± 10%, n = 126) (p = 9.9E-04) (**Fig. 4E**). This defect might reflect a role of Par3 in spindle positioning, as demonstrated in MDCK cells during cyst formation (Hao et al., 2010) (see more in DISCUSSION).

Together, the data described above suggest that Par3 defines a molecular link between cytokinesis and BC formation, and that Par3 is required for BC formation as well as its expansion by controlling tight-junction assembly and spindle orientation.

Exocyst is required for apical lumen formation

The observation that Exo70 first concentrates at the center of the tight-junction disc and then at the BC membrane (**Fig. 2B**) suggests that targeted exocytosis might drive BC formation. To test this possibility, we performed siRNA knockdown of Sec8, another subunit of the exocyst, which displayed a similar localization profile as Exo70 (**cf. Fig. 6B**), and examined its consequences in BC formation. Sec8 was knocked down effectively by the siRNA (**Fig. 5D**). BC formation was severely defective in the siSec8 cells as compared to the control cells (**Figs. 5A-C; 4A, B**). The number of cells engaged in BC formation was reduced from 80 ± 2% (n = 1781 from 3 independent experiments) for the control (siCon) cells (**Fig. 4B, left**) to 43 ± 4% (n = 1357 from 3 independent experiments) for the siSec8 cells ($p < 0.001$) (**Fig. 5B**). Sec8 knockdown also caused a significant reduction in the average length per BC, going from 13 ± 10 μm for the siCon cells (645 BCs for the 1781 cells) to 8 ± 5 μm for the siSec8 cells (295 BCs for the 1357 cells) ($p < 0.001$) (**Fig. 5C**). These phenotypes are clearly more penetrant than those displayed by the siPar3 cells (compare **Figs. 5A-C; 4A, B**), suggesting that exocytosis may be required not only for BC formation but also for its maintenance. Furthermore, siSec8 cells were noticeably more flat and spread out than either the control or the siPar3 cells. Tight junctions were formed in the siSec8 cells but they were located at the entire border between neighboring cells (**unpublished data**), resembling those of MDCK cells in 2D cultures (Gonzalez-Mariscal et al., 1985; McNeil et al., 2006). Together, these data indicate that the exocyst plays an important role in the emergence and expansion of a BC structure by promoting apical exocytosis.

Microtubules are required for the apical localization of the exocyst

To determine how apical exocytosis is targeted to the center of a disc-shaped tight junction to drive BC formation (**Fig. 2**), we examined the role of cytoskeleton in this process, as microtubules and actin filaments are known to mediate long- and short-range vesicle transport

in diverse systems, respectively (Bretscher, 2003; Caviston and Holzbaur, 2006). In post-mitotic Can 10 cells, actin filaments are localized throughout the cell cortex but highly enriched in the region surrounding the BC (**Fig. 6A; supplementary material Fig. S2**). Electron microscopic (EM) and other studies (Ishii et al., 1991; Tsukada et al., 1995) indicate that there are three distinct populations of actin filaments near the BC: those associated with the tight junctions, those inside the filopodia associated with the BC membrane, and those in an actomyosin (myosin-II) network surrounding the BC that may be responsible for the contraction and dynamics of the BC membrane. In contrast, microtubules are organized into dense networks throughout the cell periphery but do not appear to be selectively enriched at the BC region (**Fig. 6A; supplementary material Fig. S2**) (Decaens et al., 2008). When Can 10 cells were treated with 20 μM latrunculin A (LatA) for 1 hour, all actin filaments, except very few in the BC region, were disrupted (**Fig. 6A; supplementary material Fig. S2**). BCs remained but their shapes were profoundly altered, changing from the normal ball-shaped BCs (**Fig. 2A**) in non-treated cells to a variety of convoluted and/or fragmented BC structures in treated cells (**supplementary material Fig. S3**). The exocyst subunit Sec8 was still clustered at the BC region but displayed a distribution pattern that presumably reflects the underlying change in BC shape or structure (**Fig. 6B, C**) [Sec8 signal intensity around the BC is 100 ± 26% (n = 19) for the control, and 112 ± 22% (n = 20) for the LatA-treated cells; p = 0.113]. As expected, treatment of Can 10 cells with 40 μM Nocodazole (NZ) for 1 hour effectively disrupted microtubules while leaving the actin cytoskeleton and existing BCs intact (**Fig. 6A; supplementary material Fig. S2**). Remarkably, Sec8 localization at the BC region was nearly abolished (**Fig. 6B, C**) [Sec8 signal intensity around the BC is 20 ± 21% (n=19) for the NZ-treated cells; p = 1.31E-12]. A similar result was obtained with another exocyst subunit Exo70 (**Fig. 6D**) [Exo70 signal intensity around the BC is 100 ± 28% (n = 20) for the control, and 25 ± 10% (n = 10) for the NZ-treated cells; p = 5.25E-14]. These data indicate that microtubules are required for exocyst localization whereas the actin cytoskeleton is required for maintaining BC architecture.

We also observed that in addition to its accumulation at the BC (**Fig. 6E, top, arrowhead**), Exo70 also localized to other cell-cell contact regions (**Fig. 6E, top, arrow**). However, NZ

treatment selectively eliminated Exo70 localization at the BC but not other locations, suggesting that microtubules are specifically required for the apical localization of the exocyst. These data also imply that microtubules are involved in polarized transport of apical vesicles during BC formation. Because of the high density and complex organization pattern of MTs in the cortical region of Can 10 cells, it is difficult to visualize a distinct array of MTs associated with the BC membrane. To further define the role of microtubule in BC formation, we first examined the location of the centrosomes, as they are found to be near the apical membrane in some other epithelial cells and are thought to play a role in apical lumen formation, although the underlying mechanism remains unknown (Feldman and Priess, 2012; Rodriguez-Fraticelli et al., 2012). We found that at the pre-BC stage, the centrosomes, as indicated by immuno-staining of centriolin, a centrosomal protein that binds specifically to mother centriole (Gromley et al., 2005), were localized near the disc-shaped tight junctions in some cells (**supplementary material Fig. S4, top**). At the small- and large-BC stages, the centrosomes were invariably close to the BC structure (**supplementary material Fig. S4, middle and bottom; Fig. 6F**). These data suggest that after cytokinesis, the centrosomes must migrate from the spindle poles to the cell division site to orchestrate other cellular functions such as BC formation. These data are also consistent with the previous finding that γ-tubulin, another component of the centrosomes, is also localized near the tBC membrane (Decaens et al., 2008). EB1, a protein that tracks the plus ends of dynamic MTs (Akhmanova and Steinmetz, 2010; Tirnauer and Bierer, 2000), was distributed throughout the cell cortex but apparently enriched near the BC membrane (**Fig. 6G**). Together, these data suggest that an array of microtubules originated from the nearby centrosomes is engaged in exocyst-mediated apical exocytosis to drive BC formation.

Discussion

Cytokinesis defines a spatial landmark for the emergence of hepatocyte polarity and apical lumen formation

Based on this study, we propose that cytokinesis defines a spatial landmark for hepatocyte polarization and BC formation. Our "cytokinesis-landmark model" (**Fig. 7A**) posits that during the terminal phase of cytokinesis (represented by the "green" microtubule arrays at the midbody stage) (**Step1**), the key polarity regulator Par3 ("red") and the tight junction-associated protein ZO-1 ("red") are delivered to the division site sequentially before the completion of cytokinesis, presumably in preparation for subsequent BC formation. Centrosomes ("black circles") are instructed to migrate ("black arrows") close to the disc-shaped tight junctions between the daughter cells. After cytokinesis, microtubules ("purple lines" with marked + and – ends) (**Steps 2 and 3**), likely originated from the nearby centrosomes, are specifically required for exocyst localization at the BC membrane ("blue oval") and are presumably involved in targeted exocytosis of apical vesicles ("blue lines" near the centrosomes; **Step2**) to drive BC emergence (**Step 2**) and expansion (**Step 3**). While this manuscript was in revision, *de novo* BC formation was also reported to occur at the site of abscission in HepG2 cells (Slim et al., 2013). Thus, our "cytokinesis-landmark model" applies to both rat and human hepatocytes.

With this conceptual framework established (**Fig. 7A**), major mechanistic questions regarding hepatocyte polarization and BC formation can be formulated and addressed in the future using the Can 10 model. For example, we have shown that Par3 localizes to the division site before the completion of cytokinesis and is required for tight-junction assembly and BC formation after cytokinesis. Thus, Par3 is ideally positioned to convey the spatial cue from the cytokinesis machinery to enable cell polarization and BC formation at the right time and right place. However, it remains unknown how Par3 is delivered to the division site and how it regulates tight-junction assembly at the molecular level. According to the cytokinesis-landmark model (**Fig. 7A**), the centrosomes must migrate from the spindle poles to a BC-proximal region to nucleate microtubules that guide exocyst-dependent exocytosis.

However, it remains unknown how centrosome migration occurs, how microtubules interact with the exocyst or exocyst-decorated apical vesicles, and what Rab GTPase(s) and motor proteins are involved in apical exocytosis.

Does cytokinesis-linked BC formation occur at the two-cell stage *in vivo*? For technical reasons (outlined in the Results section), we could not decipher the mechanism of cell polarization and BC formation at the two-cell stage using embryonic liver sections and light microscopic methods. However, an EM study of developing rat livers clearly indicates that tight junctions with or without an associated BC are detected earliest on day 13 (the gestation period is 21 days for rats) and are restricted to the contact site between two apposing cells (Wood, 1965), which is strikingly similar to what was observed in Can 10 cells at the two-cell stage. The EM study also indicates that tight-junction assembly precedes BC formation *in vivo*, as observed in Can 10 cells *in vitro*. The apposing cells in the EM study are likely the progeny of a cell division, because, if cell-cell contact were the only trigger for tight-junction assembly and BC formation, most of the hepatocytes in a row should be able to develop these structures with two different neighbors at the same time, which is apparently not the case (Wood, 1965).

How do hepatocytes find the center of their contact surface to initiate polarization and BC formation? This is a fundamental question regarding the geometry of hepatocyte polarization. According to our "cytokinesis-landmark model", the site of BC formation is the site of cell division, which is automatically centered between the daughter cells during cytokinesis, thus solving the geometry problem. Because of its cell-autonomous nature, the cytokinesis-linked polarization mechanism could provide a highly efficient means of BC formation during liver development and regeneration.

Oriented cell division and asymmetric cytokinesis are involved in apical tube formation

In the liver, a tBC is always sandwiched by neighboring hepatocytes. It remains completely unknown how the tBC is evolved from a round or ovoid BC formed at the two-cell stage. Based on this study, we propose a "divide-and-grow" model for tBC formation, which posits

that oriented cell division results in the incomplete "division" and partitioning of the mother BC into two daughter cells, and further "growth" of the BC in the daughters, which is driven by continued exocytosis, leads to tBC formation (**Fig. 7B**). After the first division, the two daughter cells (**Step 4**, **D1 and D2**) often enter the next cell cycle asynchronously, attesting to their cytoplasmic separation. One daughter (**D1**) undergoes the next round of division before the other (**D2**). The division is oriented with the spindle ("the solid line with a double-ended arrow") in parallel to the long axis of the existing BC (**Step 4**). The division is also asymmetric (**Step 5**) presumably due to the association of the contractile ring (**Step 4**, "brown circle") with the BC membrane. Asymmetric furrowing during cell division has been frequently observed *in vivo* for many cell types including epithelial cells due to their asymmetric attachment to the ECM or neighboring cells (Founounou et al., 2013; Guillot and Lecuit, 2013; Herszterg et al., 2013; Maddox et al., 2007). This oriented division and asymmetric cytokinesis results in the partitioning of the mother BC into the two daughter cells (**Step 5**). The midbody (indicated by the "green microtubule arrays") is associated with the BC membrane and the centrosomes migrate towards the BC structure. Similar to the two-cell stage, the centrosomes nucleate microtubules to guide exocyst-dependent apical exocytosis to drive BC growth in both daughters, as indicated by the localization of the exocyst subunits Exo70 and Sec8 on the BC membrane at the three-cell or later stages (**unpublished data**). The other daughter (**D2**) will also undergo oriented cell division and asymmetric cytokinesis as the first daughter does (**Step5**, dashed spindle and contractile ring) and contribute to the overall expansion of the shared BC along the spindle axis. Repeated oriented divisions along the same direction will lead to two rows of hepatocytes sharing a central tBC with centrosomes located next to the BC membrane (**Step 6**). This is exactly the pattern of organization observed in Can 10 cells using the Mdr antibody to visualize the tBC and the centriolin (**unpublished data**) or γ-tubulin (Decaens et al., 2008) antibody to visualize the centrosomes. Similar to Can 10 cells, the midbody is always tightly associated with the BC membrane in developing livers (this study). In regenerating livers, the cleavage furrow of a dividing hepatocyte was also found to be associated with a BC in 28% of the cells examined (Bartles and Hubbard, 1986). These observations suggest that tBC formation may employ the same mechanism *in vitro* and *in vivo*. However, a recent paper reports that in regenerating mouse

livers, weaned rat livers, and HepG2 cells, the spindle axis is largely perpendicular to the BC lumen such that cell division results in asymmetric inheritance of the existing BC by the daughter cells (Slim et al., 2013). The authors hypothesize that this mode of oriented cell division, coupled with *de novo* BC formation at the site of abscission and further elongation and fusion of individual BCs, leads to the formation of a complex BC network as seen in primary hepatocytes cultured in high density and with the collagen or other ECM sandwich (Fu et al., 2010; Fu et al., 2011). Taken these observations together, it is possible that both modes of oriented cell divisions are involved in BC biogenesis *in vivo*. During early liver development, the parallel spindle-axis mode may be preferentially used to generate a tBC while during later liver development or regeneration, the perpendicular spindle-axis mode may be preferentially used to build a complex BC network.

How spindle orientation is controlled during tBC formation remains unknown. Par3 is required for oriented cell division during cyst formation by MDCK cells (Hao et al., 2010). It is thought to act by controlling aPKC (a component of the Par3-Par6-aPKC polarity complex) localization to the apical membrane, which phosphorylates LGN and results in its dissociation from the apical membrane, thereby inactivating the Gαi-LGN/Pins-NuMA system essential for the anchoring of spindle poles to the cell cortex. The serine/threonine kinase Par1 is also known to regulate spindle orientation in epithelial cells via pathways involving RhoA, LGN-NuMA, and the astral microtubules (Cohen et al., 2004; Lazaro-Dieguez et al., 2013). In Can 10 cells, siRNA knockdown of Par3 greatly reduces tBC formation (**Fig. 4A, B**) and the association of the midbody with the existing BC membrane (**Fig. 4E**). Both phenotypes are consistent with a role of Par3 in spindle orientation. However, in contrast to MDCK cells, aPKC is not localized to the apical membrane; instead, it co-localizes with Par3 at the tight junctions throughout BC formation (**unpublished data**). Thus, how Par3 controls spindle orientation in Can 10 cells requires further investigation. It will also be interesting to determine whether and how Par1 is involved in controlling spindle orientation in Can 10 cells.

Coupling of division to polarization and apical lumen formation appears to be broadly conserved in diverse polarization systems

Accumulating evidence suggests that coupling of division to polarization and apical lumen formation goes beyond the hepatocyte. When MDCK cells were embedded in ECM, the polarity protein Crumbs3 is delivered to the division site during cytokinesis and an apical lumen is formed between the daughter cells after the first division (Schluter et al., 2009). During cyst formation by the human intestinal Caco-2 cells in 3D cultures, aPKC is localized to the division site during cytokinesis and an apical lumen is formed there at the two-cell stage (Jaffe et al., 2008). In a remarkably similar way to Can 10, spindle orientation and asymmetric cytokinesis (cleavage furrow ingresses from basal to apical surface) play critical roles in cyst formation by the Caco-2 cells (Jaffe et al., 2008). In addition, the midbody is closely associated with the apical membrane (Jaffe et al., 2008). Similar spindle orientation and asymmetric cytokinesis are also observed in the crypt proliferative zone of mouse small intestine during normal tissue renewal (Fleming et al., 2007). Thus, oriented cell division and asymmetric cytokinesis may define a general mechanism for epithelial cell polarization and apical tube formation.

Coupling of division to polarization and apical domain formation also goes beyond epithelial cells. During neural tube formation in zebrafish, neuronal progenitors undergo mirror symmetric cell division. Par3 localizes to the cleavage furrow during cytokinesis and is then partitioned equally to the divided yet still attached daughter cells. Subsequently, an apical lumen (a part of the neural tube) is formed at the division site, sandwiched by the Par3 in both daughters (Tawk et al., 2007). In Drosophila, following cytokinesis by a neuronal precursor cell, the first neurite or apical pole, an indicator of the emergence of neuronal polarity, is formed at the Par3-decorated division site (Pollarolo et al., 2011). Thus, Par3 may communicate the spatial signal from division to polarization in systems ranging from hepatocytes to neurons.

Spatial coupling of division to polarization also exists in fungal cells. In the budding yeast *Saccharomyces cerevisiae*, the division site specifies the location for the next round of polarization or budding (equivalent to apical domain formation) (Bi and Park, 2012). Strikingly, budding can occur repetitively with the previous division site in the apiculate yeast

Saccharomycodes ludwigii (Streiblova et al., 1964), akin to the Can 10 and other cells described above. In the rod-shaped fission yeast *Schizosaccharomyces pombe*, immediately after cytokinesis, polarized cell growth always occurs at the old end first (*i.e.* the division site formed one or two generations ago) and then at both the old and new ends (the new end is generated during the last cell division) (Martin and Chang, 2005). These observations suggest that molecular memory exists at the previous division sites, which signals where to initiate polarization and cell growth. Taken together, spatial coupling of division to polarization and apical domain formation appears to be broadly conserved in diverse polarization systems.

Materials and Methods

Cell cultures and animals

Can 10 cells were cultured in Coon's modified F-12 medium (Sigma) with 5% fetal bovine serum (GIBCO). Mice were maintained in a pathogen-free environment. For timed pregnancies, the morning of the vaginal plug was designated day 0.5, and embryos were collected at indicated stages.

Antibodies and chemicals

The mouse anti-Mdr monoclonal antibody (c219) was purchased from SIGNET. Rabbit anti-Par3, rabbit anti-Aurora B, and rat anti-α-tubulin antibodies were purchased from Abcam. Mouse and rabbit anti-ZO-1 antibodies were purchased from Invitrogen. Mouse anti-Aurora B antibody was purchased from BD Biosciences. Mouse monoclonal antibodies against Exo70 and Sec8 antibodies were kindly provided by Drs. Wei Guo and Shu-Chan Hsu. Rabbit anti-Actin was purchased from Sigma. All the fluorescence-labeled secondary antibodies and phalloidin were purchased from Invitrogen. Latrunculin A and Nocodazole were purchased from Wako Pure Chemical Industries and Acros organics, respectively.

siRNA knockdown

Silencer® Select Pre-Designed siRNAs against rat Par3 (s135864) and Sec8 (s138195) and the Silencer® Select Negative Control No.1 siRNA were purchased from Invitrogen. The cells were transfected with lipofectamine RNAiMAX reagent (Invitrogen) following the reverse transfection protocol. After 48 hours, the knockdown efficiency was assessed by Western blotting.

Immunofluorescence and microscopy

Cells were cultured in 35mm collagen-coated glass bottom dishes and then fixed with 4% paraformaldehyde for indirect immunofluorescence or staining with other fluorescence-labeled probes. For Mdr staining, cells were permeabilized with acetone for 2 min at 4°C. For other antibodies, cells were permeabilized with 0.25% Triton X-100. Embryonic liver tissues were

rinsed in PBS and fixed in zinc-buffered formalin (Polysciences), embedded in paraffin, and cut into sections of 5-8 μm in thickness. Sections were incubated in R-buffer A (Electron Microscopy Sciences) for antigen retrieval at 120°C using a Pickcell 2100 antigen retrieval system. Sections were then rinsed in PBS and blocked with 2% donkey serum for 1 h. After incubating with various antibodies, the cell-culture dishes and the tissue slides were imaged using the Zeiss LSM710 confocal with a 20× objective lens or 63× oil immersion lens. For phase-contrast time-lapse microscopy, cells were imaged, 4 h after passage, using a DeltaVision deconvolution microscope with a 40× lens in a CO_2 environment chamber. For the cells analyzed by time lapse and Mdr staining (**Fig. 1B**), the locations of the cells were marked before time-lapse analysis. After fixation and Mdr staining, the same cells were found and imaged by fluorescence microscopy.

Image processing and analysis

All images were processed and quantified using the Fiji software (Schindelin et al., 2012). For the quantification of the BC length, the longest diameter of round-shaped canaliculi and the longest and often curved length of tubular-shaped canaliculi were measured. For quantifying the number of cells engaged in BC formation, any cell with a clear BC membrane was considered positive.

Statistical analysis

All data represent the average ± standard deviation (SD). Statistical analysis was performed using two-sided Student's t-tests.

Author contributions

T.W. and E.B. designed experiments, analyzed the data, and wrote the manuscript, and T.W. performed the experiments. K.Y. and B.Z.S. provided the mouse liver sections and guidance for immunostaining the sections, and helped manuscript preparation. D.C. provided the Can 10 cells, discussed the results, and helped manuscript preparation.

Acknowledgments

We thank Drs. Wei Guo, Shu-Chan Hsu, Stephen Doxsey and Michael Lampson for providing antibodies; Drs. Shelly Berger, Rebecca Wells, and Ken Zaret for using their tissue-culture facilities; Dr. Andrea Stout for imaging assistance, Chenghua Yang for technical assistance, and Drs. Amin Ghabrial and Rebecca Wells and the members of Bi laboratory for discussions. Work in the Bi laboratory is supported by the National Institutes of Health (NIH) grant GM87365 and a pilot grant from the University Research Foundation, and work in the Stanger laboratory is supported by the NIH grants DK083355 and DK083111 and the Pew Charitable Trusts.

References

Akhmanova, A. and Steinmetz, M. O. (2010). Microtubule +TIPs at a glance. *J. Cell Sci.* **123**, 3415-3419.

Bartles, J. R. and Hubbard, A. L. (1986). Preservation of hepatocyte plasma membrane domains during cell division *in situ* in regenerating rat liver. *Dev. Biol.* **118**, 286-295.

Bi, E. and Park, H. O. (2012). Cell polarization and cytokinesis in budding yeast. *Genetics* **191**, 347-387.

Bretscher, A. (2003). Polarized growth and organelle segregation in yeast: the tracks, motors, and receptors. *J. Cell Biol.* **160**, 811-816.

Caviston, J. P. and Holzbaur, E. L. (2006). Microtubule motors at the intersection of trafficking and transport. *Trends Cell Biol.* **16**, 530-537.

Cohen, D., Brennwald, P. J., Rodriguez-Boulan, E. and Musch, A. (2004). Mammalian PAR-1 determines epithelial lumen polarity by organizing the microtubule cytoskeleton. *J. Cell Biol.* **164**, 717-727.

Datta, A., Bryant, D. M. and Mostov, K. E. (2011). Molecular regulation of lumen morphogenesis. *Curr. Biol.* **21**, R126-136.

Decaens, C., Durand, M., Grosse, B. and Cassio, D. (2008). Which *in vitro* models could be best used to study hepatocyte polarity? *Biol. Cell* **100**, 387-398.

Delacour-Larose, M., Molla, A., Skoufias, D. A., Margolis, R. L. and Dimitrov, S. (2004). Distinct dynamics of Aurora B and Survivin during mitosis. *Cell Cycle* **3**, 1418-1426.

Feldman, J. L. and Priess, J. R. (2012). A role for the centrosome and PAR-3 in the hand-off of MTOC function during epithelial polarization. *Curr. Biol.* **22**, 575-582.

Fleming, E. S., Zajac, M., Moschenross, D. M., Montrose, D. C., Rosenberg, D. W., Cowan, A. E. and Tirnauer, J. S. (2007). Planar spindle orientation and asymmetric cytokinesis in the mouse small intestine. *J. Histochem. Cytochem.* **55**, 1173-1180.

Founounou, N., Loyer, N. and Le Borgne, R. (2013). Septins regulate the contractility of the actomyosin ring to enable adherens junction remodeling during cytokinesis of epithelial cells. *Dev. Cell* **24**, 242-255.

Fu, D., Wakabayashi, Y., Ido, Y., Lippincott-Schwartz, J. and Arias, I. M. (2010). Regulation of bile canalicular network formation and maintenance by AMP-activated protein kinase and LKB1. *J. Cell Sci.* **123**, 3294-3302.

Fu, D., Wakabayashi, Y., Lippincott-Schwartz, J. and Arias, I. M. (2011). Bile acid stimulates hepatocyte polarization through a cAMP-Epac-MEK-LKB1-AMPK pathway. *Proc. Natl. Acad. Sci. USA* **108**, 1403-1408.

Gonzalez-Mariscal, L., Chavez de Ramirez, B. and Cereijido, M. (1985). Tight junction formation in cultured epithelial cells (MDCK). *J. Membr. Biol.* **86**, 113-125.

Gromley, A., Yeaman, C., Rosa, J., Redick, S., Chen, C. T., Mirabelle, S., Guha, M., Sillibourne, J. and Doxsey, S. J. (2005). Centriolin anchoring of exocyst and SNARE complexes at the midbody is required for secretory-vesicle-mediated abscission. *Cell* **123**, 75-87.

Gruneberg, U., Neef, R., Honda, R., Nigg, E. A. and Barr, F. A. (2004). Relocation of Aurora B from centromeres to the central spindle at the metaphase to anaphase transition requires MKlp2. *J. Cell Biol.* **166**, 167-172.

Guillot, C. and Lecuit, T. (2013). Adhesion disengagement uncouples intrinsic and extrinsic forces to drive cytokinesis in epithelial tissues. *Dev. Cell* **24**, 227-241.

Hao, Y., Du, Q., Chen, X., Zheng, Z., Balsbaugh, J. L., Maitra, S., Shabanowitz, J., Hunt, D. F. and Macara, I. G. (2010). Par3 controls epithelial spindle orientation by aPKC-mediated phosphorylation of apical Pins. *Curr. Biol.* **20**, 1809-1818.

He, B. and Guo, W. (2009). The exocyst complex in polarized exocytosis. *Curr. Opin. Cell Biol.* **21**, 537-542.

Helfrich, I., Schmitz, A., Zigrino, P., Michels, C., Haase, I., le Bivic, A., Leitges, M. and Niessen, C. M. (2007). Role of aPKC isoforms and their binding partners Par3 and Par6 in epidermal barrier formation. *J. Invest. Dermatol.* **127**, 782-791.

Herszterg, S., Leibfried, A., Bosveld, F., Martin, C. and Bellaiche, Y. (2013). Interplay between the dividing cell and its neighbors regulates adherens junction formation during cytokinesis in epithelial tissue. *Dev. Cell* **24**, 256-270.

Hirose, T., Izumi, Y., Nagashima, Y., Tamai-Nagai, Y., Kurihara, H., Sakai, T., Suzuki, Y., Yamanaka, T., Suzuki, A., Mizuno, K. et al. (2002). Involvement of ASIP/PAR-3 in the

promotion of epithelial tight junction formation. *J. Cell Sci.* **115**, 2485-2495.

Hogan, B. L. and Kolodziej, P. A. (2002). Organogenesis: molecular mechanisms of tubulogenesis. *Nat. Rev. Genet.* **3**, 513-523.

Ishii, M., Washioka, H., Tonosaki, A. and Toyota, T. (1991). Regional orientation of actin filaments in the pericanalicular cytoplasm of rat hepatocytes. *Gastroenterology* **101**, 1663-1672.

Jaffe, A. B., Kaji, N., Durgan, J. and Hall, A. (2008). Cdc42 controls spindle orientation to position the apical surface during epithelial morphogenesis. *J. Cell Biol.* **183**, 625-633.

Kung, J. W., Currie, I. S., Forbes, S. J. and Ross, J. A. (2010). Liver development, regeneration, and carcinogenesis. *J. Biomed. Biotechnol.* **2010**, 984248.

Lazaro-Dieguez, F., Cohen, D., Fernandez, D., Hodgson, L., van Ijzendoorn, S. C. and Musch, A. (2013). Par1b links lumen polarity with LGN-NuMA positioning for distinct epithelial cell division phenotypes. *J. Cell Biol.* **203**, 251-264.

Lubarsky, B. and Krasnow, M. A. (2003). Tube morphogenesis: making and shaping biological tubes. *Cell* **112**, 19-28.

Maddox, A. S., Lewellyn, L., Desai, A. and Oegema, K. (2007). Anillin and the septins promote asymmetric ingression of the cytokinetic furrow. *Dev. Cell* **12**, 827-835.

Martin, S. G. and Chang, F. (2005). New end take off: regulating cell polarity during the fission yeast cell cycle. *Cell Cycle* **4**, 1046-1049.

Martin-Belmonte, F. and Mostov, K. (2008). Regulation of cell polarity during epithelial morphogenesis. *Curr. Opin. Cell Biol.* **20**, 227-234.

McCaffrey, L. M. and Macara, I. G. (2012). Signaling Pathways in Cell Polarity. *Cold Spring Harb. Perspect. Biol.* **4: a009654**.

McNeil, E., Capaldo, C. T. and Macara, I. G. (2006). Zonula occludens-1 function in the assembly of tight junctions in Madin-Darby canine kidney epithelial cells. *Mol. Biol. Cell* **17**, 1922-1932.

Murata-Hori, M., Tatsuka, M. and Wang, Y. L. (2002). Probing the dynamics and functions of aurora B kinase in living cells during mitosis and cytokinesis. *Mol. Biol. Cell* **13**, 1099-1108.

Navarro-Alvarez, N., Soto-Gutierrez, A. and Kobayashi, N. (2010). Hepatic stem cells and

liver development. *Methods Mol. Biol.* **640**, 181-236.

Novick, P. and Guo, W. (2002). Ras family therapy: Rab, Rho and Ral talk to the exocyst. *Trends Cell Biol.* **12**, 247-249.

Peng, X., Grosse, B., Le Tiec, B., Nicolas, V., Delagebeaudeuf, C., Bedda, T., Decaens, C. and Cassio, D. (2006). How to induce non-polarized cells of hepatic origin to express typical hepatocyte polarity: generation of new highly polarized cell models with developed and functional bile canaliculi. *Cell Tissue Res.* **323**, 233-243.

Pollarolo, G., Schulz, J. G., Munck, S. and Dotti, C. G. (2011). Cytokinesis remnants define first neuronal asymmetry *in vivo*. *Nat. Neurosci.* **14**, 1525-1533.

Rodriguez-Fraticelli, A. E., Auzan, M., Alonso, M. A., Bornens, M. and Martin-Belmonte, F. (2012). Cell confinement controls centrosome positioning and lumen initiation during epithelial morphogenesis. *J. Cell Biol.* **198**, 1011-1023.

Rodriguez-Fraticelli, A. E., Galvez-Santisteban, M. and Martin-Belmonte, F. (2011). Divide and polarize: recent advances in the molecular mechanism regulating epithelial tubulogenesis. *Curr. Opin. Cell Biol.* **23**, 638-646.

Schindelin, J., Arganda-Carreras, I., Frise, E., Kaynig, V., Longair, M., Pietzsch, T., Preibisch, S., Rueden, C., Saalfeld, S., Schmid, B. et al. (2012). Fiji: an open-source platform for biological-image analysis. *Nat. Methods* **9**, 676-682.

Schluter, M. A., Pfarr, C. S., Pieczynski, J., Whiteman, E. L., Hurd, T. W., Fan, S., Liu, C. J. and Margolis, B. (2009). Trafficking of Crumbs3 during cytokinesis is crucial for lumen formation. *Mol. Biol. Cell* **20**, 4652-4663.

Slim, C. L., Lazaro-Dieguez, F., Bijlard, M., Toussaint, M. J., de Bruin, A., Du, Q., Musch, A. and van Ijzendoorn, S. C. (2013). Par1b induces asymmetric inheritance of plasma membrane domains via LGN-dependent mitotic spindle orientation in proliferating hepatocytes. *PLoS Biol.* **11**, e1001739.

St Johnston, D. and Ahringer, J. (2010). Cell polarity in eggs and epithelia: parallels and diversity. *Cell* **141**, 757-774.

Streiblova, E., Beran, K. and Pokorny, V. (1964). Multiple Scars, a New Type of Yeast Scar in Apiculate Yeasts. *J. Bacteriol.* **88**, 1104-1011.

Tawk, M., Araya, C., Lyons, D. A., Reugels, A. M., Girdler, G. C., Bayley, P. R., Hyde, D.

R., Tada, M. and Clarke, J. D. (2007). A mirror-symmetric cell division that orchestrates neuroepithelial morphogenesis. *Nature* **446**, 797-800.

Tirnauer, J. S. and Bierer, B. E. (2000). EB1 proteins regulate microtubule dynamics, cell polarity, and chromosome stability. *J. Cell Biol.* **149**, 761-766.

Treyer, A. and Musch, A. (2013). Hepatocyte polarity. *Compr. Physiol.* **3**, 243-287.

Tsukada, N., Ackerley, C. A. and Phillips, M. J. (1995). The structure and organization of the bile canalicular cytoskeleton with special reference to actin and actin-binding proteins. *Hepatology* **21**, 1106-1113.

Tuma, P. L., Finnegan, C. M., Yi, J. H. and Hubbard, A. L. (1999). Evidence for apical endocytosis in polarized hepatic cells: phosphoinositide 3-kinase inhibitors lead to the lysosomal accumulation of resident apical plasma membrane proteins. *J. Cell Biol.* **145**, 1089-1102.

Tuma, P. L., Nyasae, L. K., Backer, J. M. and Hubbard, A. L. (2001). Vps34p differentially regulates endocytosis from the apical and basolateral domains in polarized hepatic cells. *J. Cell Biol.* **154**, 1197-1208.

Wakabayashi, Y., Dutt, P., Lippincott-Schwartz, J. and Arias, I. M. (2005). Rab11a and myosin Vb are required for bile canalicular formation in WIF-B9 cells. *Proc. Natl. Acad. Sci. USA* **102**, 15087-15092.

Wang, L. and Boyer, J. L. (2004). The maintenance and generation of membrane polarity in hepatocytes. *Hepatology* **39**, 892-899.

Wood, R. L. (1965). An Electron Microscope Study of Developing Bile Canaliculi in the Rat. *Anat. Rec.* **151**, 507-529.

Zegers, M. M. and Hoekstra, D. (1998). Mechanisms and functional features of polarized membrane traffic in epithelial and hepatic cells. *Biochem. J.* **336**, 257-269.

Figure legends

Fig. 1. Cytokinesis defines a spatial landmark for hepatocyte polarization and BC formation

(**A**) Time-lapse analysis of cytokinesis and BC formation in Can 10 cells. See also **Movie 1 in supplementary material**. Time, h:min. Except where noted, scale bars represent 3 μm. (**B**) Can 10 cells were analyzed by time-lapse microscopy (See also **Movie 2 in supplementary material**), and then fixed and stained for Mdr (green, arrow). Scale bar, 10 μm. (**C**) Localization of Par3/ZO-1/Mdr (red) during different midbody stages (Aurora B, green). Arrows indicate the association between Par3 and Aurora B-decorated microtubule arrays.

Fig. 2. Assembly and opening of a disc-shaped tight junction at the division site is associated with *de novo* BC formation

(**A**) Localization of F-actin (gray) /Mdr (red) /ZO-1 (green) and morphogenesis of the tight junction (ZO-1) during different stages of BC formation in post-cytokinesis cells. All images are snap shots of 3D reconstructions (0.5 μm × 8-10 optical slices) at specific angles. Pre-BC, small-BC, and large-BC stages were defined as those displaying a single line, two lines separated by a short space, and two puncta of ZO-1 signal (side view), respectively. (**B**) Exo70 (green) localization with respect to ZO-1 (red) and F-actin (gray) during different stages of BC formation. (**C**) Co-localization of Par3 (green) and ZO-1 (red) during different stages of BC formation

Fig. 3. Oriented cell division and asymmetric cytokinesis are associated with tubular BC formation

(**A-B**) Spindle orientation (tubulin, green; each line in the bottom panel represents one measurement) (A) and asymmetric furrow ingression (B) with respect to the existing BC (F-actin, red; ZO-1, blue) during tBC formation. (**C**) New round of cell division (Aurora B, green) is associated with a constriction point (arrow) on the preexisting BC membrane (Mdr, red). Images are snap shots of 3D reconstructions (0.25 μm × 27 optical slices) at specific angles. (**D**) Tight-junction morphology (ZO-1, red) at the midbody stage (Aurora B, green)

during a new round of cell division (See also **Movie 4 in supplementary material**). Images are snap shots of a 3D reconstruction (0.45 μm × 24 optical slices) at different magnifications. Note that the two sibling hepatocytes involved in the initial BC formation do not enter the next cell cycle synchronously (Aurora B is known to decorate interphase nuclei). (**E**) New round of cell division (Aurora B, green, arrow) is also associated with the preexisting BC (ZO-1, red) in E17.5 mouse livers.

Fig. 4. Knockdown of Par3 prevents *de novo* BC formation and tubular BC extension

(**A**) Representative images of BC formation in the control (si Con) and Par3-knockdown (si Par3) cells. F-actin, red; Mdr, green. Scale bar, 10 μm. (**B**) Percentage of cells engaged in BC formation (left) and BC-length distribution (right) in the same samples as in (A) were quantified. (**C**) Distribution of BCs at early (pre-BC and perhaps small-BC) and late (large-BC) stages in the control (si Con) and Par3-knockdown (si Par3) cells. Note that these counts were based on single optical sections of cells stained for ZO-1, Par3 (no Par3 was detected at the tight junctions in the siPar3 cells), and F-actin; thus, it was difficult to distinguish the pre-BC from the small-BC stage. Therefore, they were grouped together as "early stage". However, it is important to note that more than 90% of the "early-stage" BCs in the control cells displayed a single line of ZO-1 signal, similar to that at the pre-BC stage as visualized by 3D reconstruction. (**D**) Western blotting indicates that the level of Par3 (relative molecular mass: 150 kD) in the si Par3 cells was reduced to 17% of that in the control cells. Actin was used as a loading control. (**E**) Knockdown of Par3 causes disassociation between the midbody and the preexisting BC.

Fig. 5. Exocyst is required for BC formation

(**A**) Representative image of BC formation in the Sec8-knockdown (si Sec8) cells. F-actin, red; Mdr, green. Scale bar, 10 μm. (**B-C**) Percentage of cells engaged in BC formation (B) and BC-length distribution (C) in the control (the same as in **Fig. 4A**) and siSec8 cells were quantified. (**D**) Western blotting indicates that the level of Sec8 (relative molecular mass: 110 kD) in the siSec8 cells was reduced to 22% of that in the control cells. Actin was used as a loading control.

Fig. 6. Microtubules are specifically required for the apical localization of the exocyst

(**A**) Distinct effects of latrunuculin A (LatA) and nocodazole (NZ) treatments on the actin cytoskeleton (F-actin, red), microtubules (tubulin, green), and BC architecture (ZO-1, blue). See also **supplementary material Figs. S2, S3**. (**B**) Distinct effects of LatA and NZ treatments on exocyst (Sec8, green) localization at the BC (ZO-1, red). (**C**) Quantification of Sec8 fluorescence signal around the BC in the control (Con), LatA-, and NZ-treated cells. (**D**) Quantification of Exo70 fluorescence signal around the BC in the control (Con) and NZ-treated cells. (**E**) NZ treatment specifically disrupts exocyst localization (Exo70, green) at the BC but not other cell-cell contact surfaces. F-actin, red; ZO-1, blue. (**F**) Localization of centrosomes (centriolin, green) with respect to the BC membrane (Mdr, red). See also **supplementary material Fig. S4**. (**G**) Localization of centrosomes (centriolin, green) and microtubule plus ends (EB1, red) with respect to the BC (inferred by location).

Fig. 7. Models for hepatocyte polarization and BC formation

(**A**) Cytokinesis landmark model for hepatocyte polarization and BC emergence. See text for details. (**B**) Divide-and-grow model for tBC formation. See text for details.

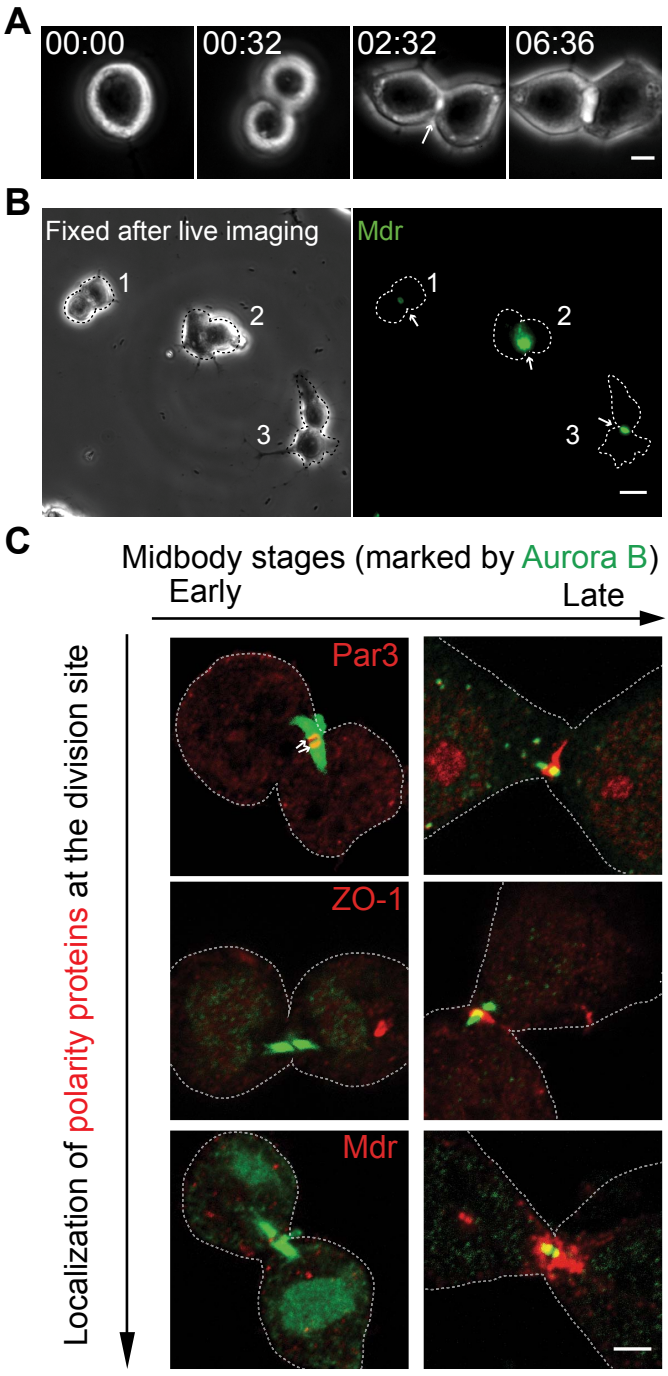

Figure 1. Wang et al.

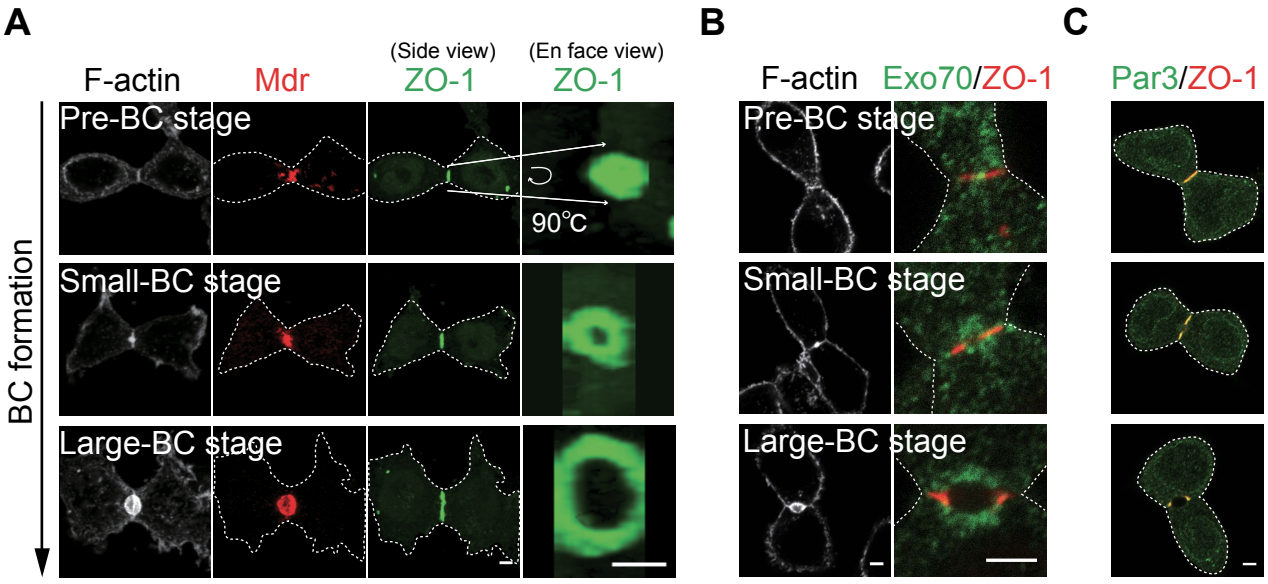

Figure 2. Wang et al.

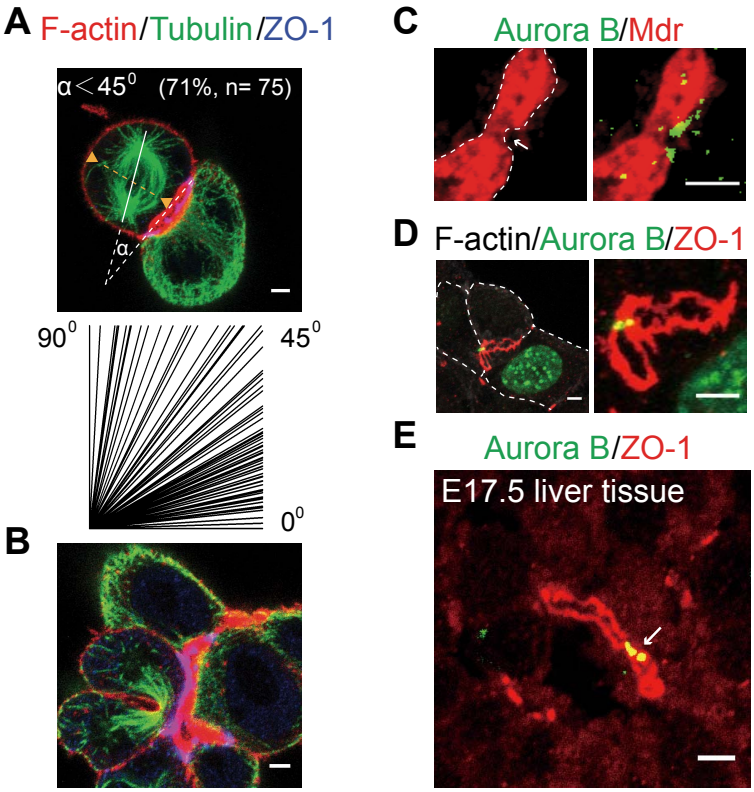

Figure 3. Wang et al.

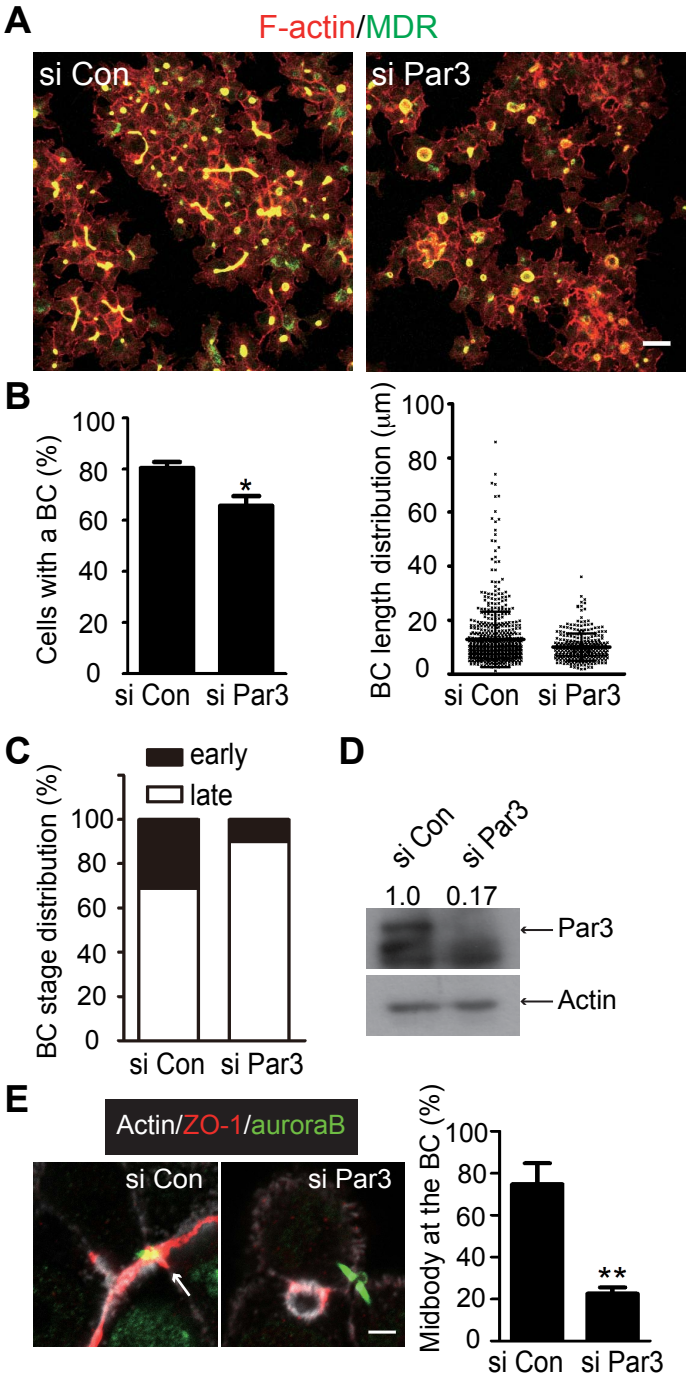

Figure 4. Wang et al.

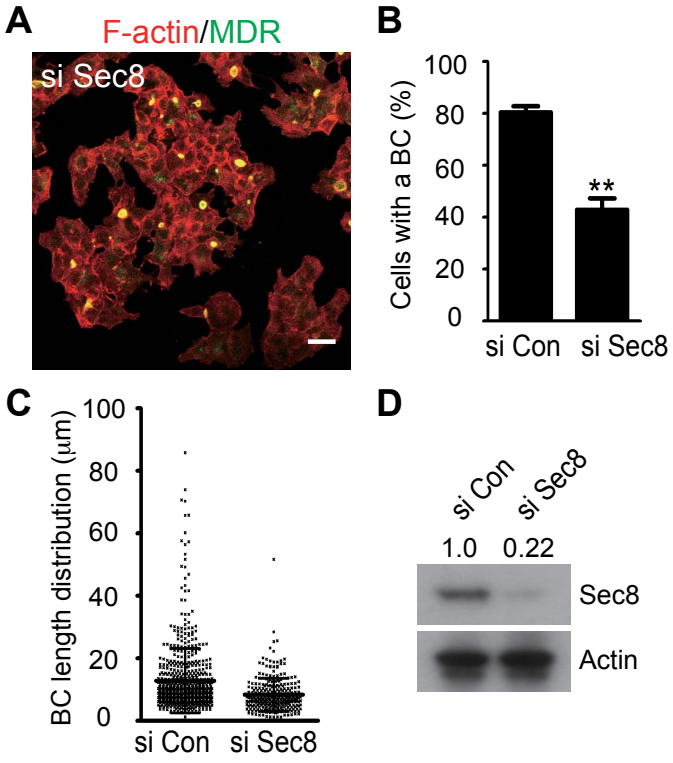

Figure 5. Wang et al.

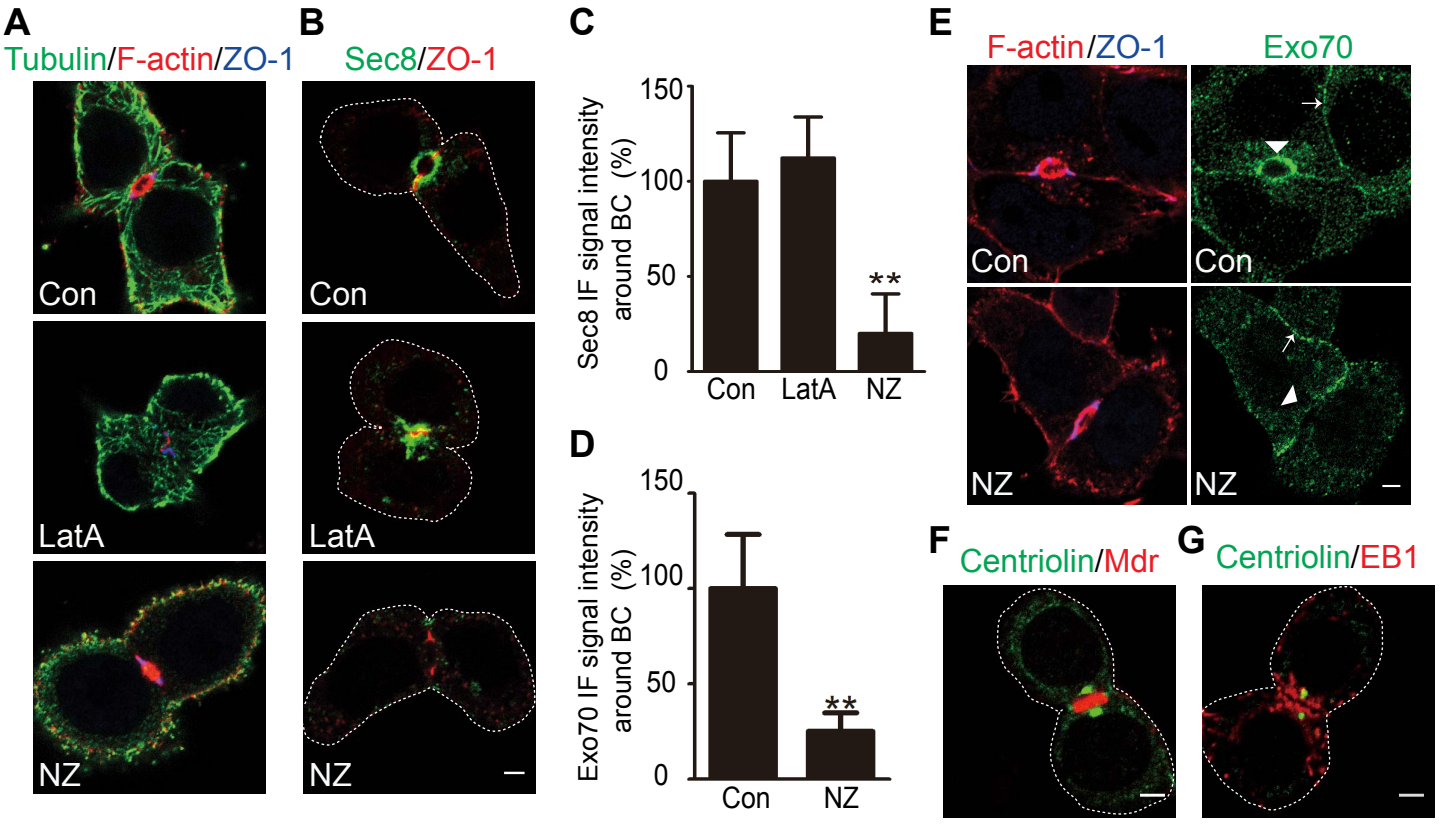

Figure 6. Wang et al.

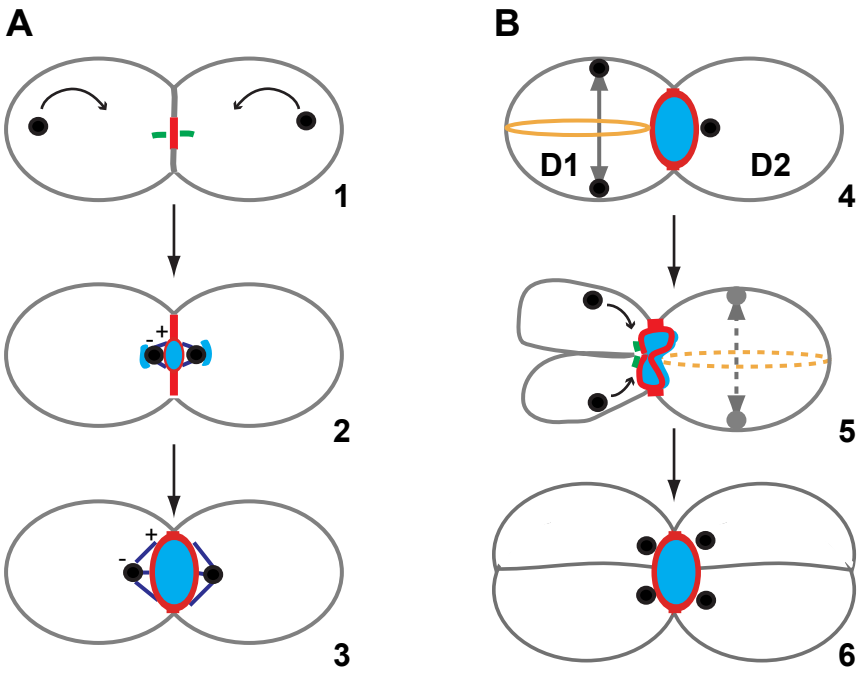

Figure 7. Wang et al.